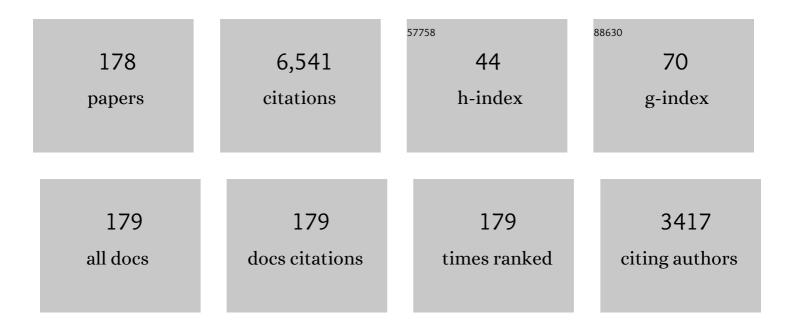
Mark A Clilverd

List of Publications by Year in descending order

Source: https://exaly.com/author-pdf/5931043/publications.pdf Version: 2024-02-01



#	Article	IF	CITATIONS
1	Solar forcing for CMIP6 (v3.2). Geoscientific Model Development, 2017, 10, 2247-2302.	3.6	293
2	Use of POES SEMâ $\in 2$ observations to examine radiation belt dynamics and energetic electron precipitation into the atmosphere. Journal of Geophysical Research, 2010, 115, .	3.3	209
3	Impact of different energies of precipitating particles on NOx generation in the middle and upper atmosphere during geomagnetic storms. Journal of Atmospheric and Solar-Terrestrial Physics, 2009, 71, 1176-1189.	1.6	166
4	Missing driver in the Sun–Earth connection from energetic electron precipitation impacts mesospheric ozone. Nature Communications, 2014, 5, 5197.	12.8	148
5	Diurnal variation of ozone depletion during the October-November 2003 solar proton events. Journal of Geophysical Research, 2005, 110, .	3.3	147
6	Geomagnetic activity and polar surface air temperature variability. Journal of Geophysical Research, 2009, 114, .	3.3	135
7	Energetic electron precipitation associated with pulsating aurora: EISCAT and Van Allen Probe observations. Journal of Geophysical Research: Space Physics, 2015, 120, 2754-2766.	2.4	133
8	Large solar flares and their ionosphericDregion enhancements. Journal of Geophysical Research, 2005, 110, .	3.3	131
9	Origins of plasmaspheric hiss. Journal of Geophysical Research, 2006, 111, .	3.3	118
10	Geomagnetic activity related NO _x enhancements and polar surface air temperature variability in a chemistry climate model: modulation of the NAM index. Atmospheric Chemistry and Physics, 2011, 11, 4521-4531.	4.9	118
11	Solar flare induced ionospheric D-region enhancements from VLF amplitude observations. Journal of Atmospheric and Solar-Terrestrial Physics, 2001, 63, 1729-1737.	1.6	106
12	Remote sensing space weather events: Antarcticâ€Arctic Radiationâ€belt (Dynamic) Depositionâ€VLF Atmospheric Research Konsortium network. Space Weather, 2009, 7, .	3.7	102
13	Observations of coincident EMIC wave activity and duskside energetic electron precipitation on 18–19 January 2013. Geophysical Research Letters, 2015, 42, 5727-5735.	4.0	102
14	Monitoring spatial and temporal variations in the dayside plasmasphere using geomagnetic field line resonances. Journal of Geophysical Research, 1999, 104, 19955-19969.	3.3	100
15	Arctic and Antarctic polar winter NOxand energetic particle precipitation in 2002–2006. Geophysical Research Letters, 2007, 34, .	4.0	97
16	Geomagnetic activity signatures in wintertime stratosphere wind, temperature, and wave response. Journal of Geophysical Research D: Atmospheres, 2013, 118, 2169-2183.	3.3	95
17	Observations of relativistic electron precipitation from the radiation belts driven by EMIC waves. Geophysical Research Letters, 2008, 35, .	4.0	93
18	Nighttime ionospheric <i>D</i> region parameters from VLF phase and amplitude. Journal of Geophysical Research, 2007, 112, .	3.3	87

#	Article	IF	CITATIONS
19	POES satellite observations of EMICâ€wave driven relativistic electron precipitation during 1998–2010. Journal of Geophysical Research: Space Physics, 2013, 118, 232-243.	2.4	87
20	Total solar eclipse effects on VLF signals: Observations and modeling. Radio Science, 2001, 36, 773-788.	1.6	86
21	Contrasting the efficiency of radiation belt losses caused by ducted and nonducted whistlerâ€mode waves from groundâ€based transmitters. Journal of Geophysical Research, 2010, 115, .	3.3	79
22	The Balloon Array for RBSP Relativistic Electron Losses (BARREL). Space Science Reviews, 2013, 179, 503-530.	8.1	76
23	Destruction of the tertiary ozone maximum during a solar proton event. Geophysical Research Letters, 2006, 33, .	4.0	75
24	Radiation belt electron precipitation into the atmosphere: Recovery from a geomagnetic storm. Journal of Geophysical Research, 2007, 112, .	3.3	75
25	First evidence of mesospheric hydroxyl response to electron precipitation from the radiation belts. Journal of Geophysical Research, 2011, 116, .	3.3	75
26	Radiation belt electron precipitation by manâ€made VLF transmissions. Journal of Geophysical Research, 2008, 113, .	3.3	73
27	Evidence of subâ€MeV EMICâ€driven electron precipitation. Geophysical Research Letters, 2017, 44, 1210-1218.	4.0	66
28	World-wide lightning location using VLF propagation in the Earth-ionosphere waveguide. IEEE Antennas and Propagation Magazine, 2008, 50, 40-60.	1.4	65
29	Electron precipitation from EMIC waves: A case study from 31 May 2013. Journal of Geophysical Research: Space Physics, 2015, 120, 3618-3631.	2.4	65
30	Comparison between POES energetic electron precipitation observations and riometer absorptions: Implications for determining true precipitation fluxes. Journal of Geophysical Research: Space Physics, 2013, 118, 7810-7821.	2.4	63
31	A model providing longâ€ŧerm data sets of energetic electron precipitation during geomagnetic storms. Journal of Geophysical Research D: Atmospheres, 2016, 121, 12,520.	3.3	63
32	Sunrise effects on VLF signals propagating over a long north-south path. Radio Science, 1999, 34, 939-948.	1.6	62
33	Groundâ€based transmitter signals observed from space: Ducted or nonducted?. Journal of Geophysical Research, 2008, 113, .	3.3	60
34	Highâ€resolution in situ observations of electron precipitationâ€causing EMIC waves. Geophysical Research Letters, 2015, 42, 9633-9641.	4.0	59
35	Precipitating radiation belt electrons and enhancements of mesospheric hydroxyl during 2004–2009. Journal of Geophysical Research, 2012, 117, .	3.3	54
36	Significance of lightning-generated whistlers to inner radiation belt electron lifetimes. Journal of Geophysical Research, 2003, 108, .	3.3	53

#	Article	IF	CITATIONS
37	Contrasting the responses of three different groundâ€based instruments to energetic electron precipitation. Radio Science, 2012, 47, .	1.6	53
38	Substormâ€induced energetic electron precipitation: Impact on atmospheric chemistry. Geophysical Research Letters, 2015, 42, 8172-8176.	4.0	51
39	Groundâ€based estimates of outer radiation belt energetic electron precipitation fluxes into the atmosphere. Journal of Geophysical Research, 2010, 115, .	3.3	50
40	The plasmasphere during a space weather event: first results from the PLASMON project. Journal of Space Weather and Space Climate, 2013, 3, A23.	3.3	50
41	Geomagnetic perturbations on stratospheric circulation in late winter and spring. Journal of Geophysical Research, 2008, 113, .	3.3	49
42	Longâ€Lasting Geomagnetically Induced Currents and Harmonic Distortion Observed in New Zealand During the 7–8 September 2017 Disturbed Period. Space Weather, 2018, 16, 704-717.	3.7	48
43	The effects of hardâ€spectra solar proton events on the middle atmosphere. Journal of Geophysical Research, 2008, 113, .	3.3	47
44	Predicting Solar Cycle 24 and beyond. Space Weather, 2006, 4, n/a-n/a.	3.7	46
45	NO _x enhancements in the middle atmosphere during 2003–2004 polar winter: Relative significance of solar proton events and the aurora as a source. Journal of Geophysical Research, 2007, 112, .	3.3	45
46	Daytime midlatitude <i>D</i> region parameters at solar minimum from short-path VLF phase and amplitude. Journal of Geophysical Research, 2011, 116, .	3.3	45
47	Longâ€Term Geomagnetically Induced Current Observations From New Zealand: Peak Current Estimates for Extreme Geomagnetic Storms. Space Weather, 2017, 15, 1447-1460.	3.7	44
48	Dynamic geomagnetic rigidity cutoff variations during a solar proton event. Journal of Geophysical Research, 2006, 111, .	3.3	43
49	Confirmation of EMIC waveâ€driven relativistic electron precipitation. Journal of Geophysical Research: Space Physics, 2016, 121, 5366-5383.	2.4	43
50	Longâ€ŧerm geomagnetically induced current observations in New Zealand: Earth return corrections and geomagnetic field driver. Space Weather, 2017, 15, 1020-1038.	3.7	43
51	Nature's Grand Experiment: Linkage between magnetospheric convection and the radiation belts. Journal of Geophysical Research: Space Physics, 2016, 121, 171-189.	2.4	42
52	Modeling a large solar proton event in the southern polar atmosphere. Journal of Geophysical Research, 2005, 110, .	3.3	41
53	Determining the spectra of radiation belt electron losses: Fitting DEMETER electron flux observations for typical and storm times. Journal of Geophysical Research: Space Physics, 2013, 118, 7611-7623.	2.4	41
54	Solar cycle changes in daytime VLF subionospheric attenuation. Journal of Atmospheric and Solar-Terrestrial Physics, 2000, 62, 601-608.	1.6	40

#	Article	IF	CITATIONS
55	Longitudinal hotspots in the mesospheric OH variations due to energetic electron precipitation. Atmospheric Chemistry and Physics, 2014, 14, 1095-1105.	4.9	40
56	An Investigation of VLF Transmitter Wave Power in the Inner Radiation Belt and Slot Region. Journal of Geophysical Research: Space Physics, 2019, 124, 5246-5259.	2.4	40
57	Reconstructing the long-termaaindex. Journal of Geophysical Research, 2005, 110, .	3.3	39
58	Ionospheric evidence of thermosphere-to-stratosphere descent of polar NOX. Geophysical Research Letters, 2006, 33, .	4.0	39
59	Energetic electron precipitation during substorm injection events: High″atitude fluxes and an unexpected midlatitude signature. Journal of Geophysical Research, 2008, 113, .	3.3	39
60	Direct observations of nitric oxide produced by energetic electron precipitation into the Antarctic middle atmosphere. Geophysical Research Letters, 2011, 38, n/a-n/a.	4.0	38
61	Polar Ozone Response to Energetic Particle Precipitation Over Decadal Time Scales: The Role of Mediumâ€Energy Electrons. Journal of Geophysical Research D: Atmospheres, 2018, 123, 607-622.	3.3	38
62	Occurrence characteristics of relativistic electron microbursts from SAMPEX observations. Journal of Geophysical Research: Space Physics, 2017, 122, 8096-8107.	2.4	37
63	An Updated Model Providing Longâ€Term Data Sets of Energetic Electron Precipitation, Including Zonal Dependence. Journal of Geophysical Research D: Atmospheres, 2018, 123, 9891-9915.	3.3	37
64	The Role of Localized Compressional Ultraâ€low Frequency Waves in Energetic Electron Precipitation. Journal of Geophysical Research: Space Physics, 2018, 123, 1900-1914.	2.4	36
65	The importance of atmospheric precipitation in storm-time relativistic electron flux drop outs. Geophysical Research Letters, 2006, 33, n/a-n/a.	4.0	35
66	Prediction of relativistic electron flux at geostationary orbit following storms: Multiple regression analysis. Journal of Geophysical Research: Space Physics, 2014, 119, 7297-7318.	2.4	35
67	Substormâ€induced energetic electron precipitation: Morphology and prediction. Journal of Geophysical Research: Space Physics, 2015, 120, 2993-3008.	2.4	34
68	Empirical predictive models of daily relativistic electron flux at geostationary orbit: Multiple regression analysis. Journal of Geophysical Research: Space Physics, 2016, 121, 3181-3197.	2.4	34
69	The causes of long-term change in theaaindex. Journal of Geophysical Research, 2002, 107, SSH 4-1-SSH 4-7.	3.3	33
70	Energetic particle precipitation into the middle atmosphere triggered by a coronal mass ejection. Journal of Geophysical Research, 2007, 112, .	3.3	33
71	Effects of VLF Transmitter Waves on the Inner Belt and Slot Region. Journal of Geophysical Research: Space Physics, 2019, 124, 5260-5277.	2.4	33
72	Determining the size of lightning-induced electron precipitation patches. Journal of Geophysical Research, 2002, 107, SIA 10-1-SIA 10-11.	3.3	32

5

#	Article	IF	CITATIONS
73	Modeling polar ionospheric effects during the October-November 2003 solar proton events. Radio Science, 2006, 41, n/a-n/a.	1.6	32
74	Significance of transient luminous events to neutral chemistry: Experimental measurements. Geophysical Research Letters, 2008, 35, .	4.0	31
75	Radiation belt electron precipitation due to geomagnetic storms: Significance to middle atmosphere ozone chemistry. Journal of Geophysical Research, 2010, 115, .	3.3	31
76	Investigating energetic electron precipitation through combining groundâ€based and balloon observations. Journal of Geophysical Research: Space Physics, 2017, 122, 534-546.	2.4	31
77	Solar activity levels in 2100. Astronomy and Geophysics, 2003, 44, 5.20-5.22.	0.2	30
78	Additional stratospheric NO _{<i>x</i>} production by relativistic electron precipitation during the 2004 spring NO _{<i>x</i>} descent event. Journal of Geophysical Research, 2009, 114, .	3.3	29
79	Longâ€ŧerm determination of energetic electron precipitation into the atmosphere from AARDDVARK subionospheric VLF observations. Journal of Geophysical Research: Space Physics, 2015, 120, 2194-2211.	2.4	29
80	Energetic particle injection, acceleration, and loss during the geomagnetic disturbances which upset Galaxy 15. Journal of Geophysical Research, 2012, 117, .	3.3	28
81	A reexamination of latitudinal limits of substormâ€produced energetic electron precipitation. Journal of Geophysical Research: Space Physics, 2013, 118, 6694-6705.	2.4	28
82	Relativistic microburst storm characteristics: Combined satellite and groundâ€based observations. Journal of Geophysical Research, 2010, 115, .	3.3	27
83	Energetic particle forcing of the Northern Hemisphere winter stratosphere: comparison to solar irradiance forcing. Frontiers in Physics, 2014, 2, .	2.1	27
84	Temporal variability of the descent of highâ€altitude NO _X inferred from ionospheric data. Journal of Geophysical Research, 2007, 112, .	3.3	26
85	Atmospheric impact of the Carrington event solar protons. Journal of Geophysical Research, 2008, 113,	3.3	25
86	Lower-thermosphere–ionosphere (LTI) quantities: current status of measuring techniques and models. Annales Geophysicae, 2021, 39, 189-237.	1.6	25
87	Lightning-driven inner radiation belt energy deposition into the atmosphere: implications for ionisation-levels and neutral chemistry. Annales Geophysicae, 2007, 25, 1745-1757.	1.6	25
88	Daedalus: a low-flying spacecraft for in situ exploration of the lower thermosphere–ionosphere. Geoscientific Instrumentation, Methods and Data Systems, 2020, 9, 153-191.	1.6	25
89	In situ and ground-based intercalibration measurements of plasma density atL= 2.5. Journal of Geophysical Research, 2003, 108, .	3.3	24
90	Longitudinal and seasonal variations in plasmaspheric electron density: Implications for electron precipitation. Journal of Geophysical Research, 2007, 112, .	3.3	24

#	Article	IF	CITATIONS
91	Lowâ€ŀatitude ionospheric <i>D</i> region dependence on solar zenith angle. Journal of Geophysical Research: Space Physics, 2014, 119, 6865-6875.	2.4	24
92	Relativistic Electron Microburst Events: Modeling the Atmospheric Impact. Geophysical Research Letters, 2018, 45, 1141-1147.	4.0	23
93	Plasmaspheric storm time erosion. Journal of Geophysical Research, 2000, 105, 12997-13008.	3.3	22
94	Storm time, shortâ€lived bursts of relativistic electron precipitation detected by subionospheric radio wave propagation. Journal of Geophysical Research, 2007, 112, .	3.3	22
95	Source region for whistlers detected at Rothera, Antarctica. Journal of Geophysical Research, 2011, 116, .	3.3	22
96	Observations and Modeling of Increased Nitric Oxide in the Antarctic Polar Middle Atmosphere Associated With Geomagnetic Stormâ€Driven Energetic Electron Precipitation. Journal of Geophysical Research: Space Physics, 2018, 123, 6009-6025.	2.4	22
97	Rapid Radiation Belt Losses Occurring During High-Speed Solar Wind Stream-Driven Storms: Importance of Energetic Electron Precipitation. Geophysical Monograph Series, 2013, , 213-224.	0.1	21
98	Nonlinear and Synergistic Effects of ULF Pc5, VLF Chorus, and EMIC Waves on Relativistic Electron Flux at Geosynchronous Orbit. Journal of Geophysical Research: Space Physics, 2018, 123, 4755-4766.	2.4	21
99	Ground-based evidence of latitude-dependent cyclotron absorption of whistler mode signals originating from VLF transmitters. Journal of Geophysical Research, 1996, 101, 2355-2367.	3.3	20
100	The atmospheric implications of radiation belt remediation. Annales Geophysicae, 2006, 24, 2025-2041.	1.6	20
101	Energetic electron precipitation and auroral morphology at the substorm recovery phase. Journal of Geophysical Research: Space Physics, 2017, 122, 6508-6527.	2.4	20
102	A Distributed Lag Autoregressive Model of Geostationary Relativistic Electron Fluxes: Comparing the Influences of Waves, Seed and Source Electrons, and Solar Wind Inputs. Journal of Geophysical Research: Space Physics, 2018, 123, 3646-3671.	2.4	20
103	Characteristics of Relativistic Microburst Intensity From SAMPEX Observations. Journal of Geophysical Research: Space Physics, 2019, 124, 5627-5640.	2.4	20
104	Midlatitude ionospheric <i>D</i> region: Height, sharpness, and solar zenith angle. Journal of Geophysical Research: Space Physics, 2017, 122, 8933-8946.	2.4	19
105	Geomagnetically Induced Currents and Harmonic Distortion: Stormâ€Time Observations From New Zealand. Space Weather, 2020, 18, e2019SW002387.	3.7	19
106	Latitudinally dependent Trimpi effects: Modeling and observations. Journal of Geophysical Research, 1999, 104, 19881-19887.	3.3	18
107	Inner radiation belt electron lifetimes due to whistler-induced electron precipitation (WEP) driven losses. Geophysical Research Letters, 2002, 29, 30-1-30-4.	4.0	17
108	Radiation belt electron precipitation fluxes associated with lightning. Journal of Geophysical Research, 2004, 109, .	3.3	17

#	Article	IF	CITATIONS
109	The effects and correction of the geometric factor for the POES/MEPED electron flux instrument using a multisatellite comparison. Journal of Geophysical Research: Space Physics, 2014, 119, 6386-6404.	2.4	17
110	Comparing Electron Precipitation Fluxes Calculated From Pitch Angle Diffusion Coefficients to LEO Satellite Observations. Journal of Geophysical Research: Space Physics, 2021, 126, e2020JA028410.	2.4	17
111	Testing the importance of precipitation loss mechanisms in the inner radiation belt. Geophysical Research Letters, 2004, 31, n/a-n/a.	4.0	16
112	Automatic Whistler Detector and Analyzer system: Implementation of the analyzer algorithm. Journal of Geophysical Research, 2010, 115, .	3.3	16
113	The annual and longitudinal variations in plasmaspheric ion density. Journal of Geophysical Research, 2012, 117, .	3.3	16
114	Characteristics of precipitating energetic electron fluxes relative to the plasmapause during geomagnetic storms. Journal of Geophysical Research: Space Physics, 2014, 119, 8784-8800.	2.4	16
115	<i>D</i> -region ion–neutral coupled chemistry (Sodankyläon Chemistry,) Tj E WACCM-rSIC. Geoscientific Model Development, 2016, 9, 3123-3136.	TQq1 1 0.7 3.6	′84314 rgB 16
116	HEPPA III Intercomparison Experiment on Electron Precipitation Impacts: 1. Estimated Ionization Rates During a Geomagnetic Active Period in April 2010. Journal of Geophysical Research: Space Physics, 2022, 127, .	2.4	16
117	Characteristics of localized ionospheric disturbances inferred from VLF measurements at two closely spaced receivers. Journal of Geophysical Research, 1996, 101, 15737-15747.	3.3	15
118	Energetic outer radiation belt electron precipitation during recurrent solar activity. Journal of Geophysical Research, 2010, 115, .	3.3	15
119	Daytime <i>D</i> region parameters from long-path VLF phase and amplitude. Journal of Geophysical Research, 2011, 116, n/a-n/a.	3.3	15
120	Comparison of Relativistic Microburst Activity Seen by SAMPEX With Groundâ€Based Wave Measurements at Halley, Antarctica. Journal of Geophysical Research: Space Physics, 2018, 123, 1279-1294.	2.4	15
121	Lightning driven inner radiation belt energy deposition into the atmosphere: regional and global estimates. Annales Geophysicae, 2005, 23, 3419-3430.	1.6	13
122	Hiss from the chorus. Nature, 2008, 452, 41-42.	27.8	13
123	Combined THEMIS and groundâ€based observations of a pair of substormâ€associated electron precipitation events. Journal of Geophysical Research, 2012, 117, .	3.3	13
124	A case study of electron precipitation fluxes due to plasmaspheric hiss. Journal of Geophysical Research: Space Physics, 2015, 120, 6736-6748.	2.4	13
125	Northern Hemisphere Stratospheric Ozone Depletion Caused by Solar Proton Events: The Role of the Polar Vortex. Geophysical Research Letters, 2018, 45, 2115-2124.	4.0	13
126	Geomagnetically Induced Currents and Harmonic Distortion: High Time Resolution Case Studies. Space Weather, 2020, 18, e2020SW002594.	3.7	13

#	Article	IF	CITATIONS
127	Improved dynamic geomagnetic rigidity cutoff modeling: Testing predictive accuracy. Journal of Geophysical Research, 2007, 112, .	3.3	12
128	Simultaneous observation of chorus and hiss near the plasmapause. Journal of Geophysical Research, 2012, 117, .	3.3	12
129	Analysis of the effectiveness of groundâ€based VLF wave observations for predicting or nowcasting relativistic electron flux at geostationary orbit. Journal of Geophysical Research: Space Physics, 2015, 120, 2052-2060.	2.4	12
130	Mesospheric Nitric Acid Enhancements During Energetic Electron Precipitation Events Simulated by WACCMâ€Ð. Journal of Geophysical Research D: Atmospheres, 2018, 123, 6984-6998.	3.3	12
131	Developing a Nowcasting Capability for Xâ€Class Solar Flares Using VLF Radiowave Propagation Changes Space Weather, 2019, 17, 1783-1799.	3.7	12
132	A statistical approach to determining energetic outer radiation belt electron precipitation fluxes. Journal of Geophysical Research: Space Physics, 2014, 119, 3961-3978.	2.4	11
133	Geomagnetically induced currents during the 07–08 September 2017 disturbed period: a global perspective. Journal of Space Weather and Space Climate, 2021, 11, 33.	3.3	11
134	Geomagnetically Induced Current Model in New Zealand Across Multiple Disturbances: Validation and Extension to Nonâ€Monitored Transformers. Space Weather, 2022, 20, .	3.7	11
135	Dregion reflection height modification by whistler-induced electron precipitation. Journal of Geophysical Research, 2002, 107, SIA 18-1.	3.3	10
136	A Multiâ€Instrument Approach to Determining the Sourceâ€Region Extent of EEPâ€Driving EMIC Waves. Geophysical Research Letters, 2020, 47, e2019GL086599.	4.0	10
137	Energetic electron precipitation characteristics observed from Antarctica during a flux dropout event. Journal of Geophysical Research: Space Physics, 2013, 118, 6921-6935.	2.4	9
138	Observations of nitric oxide in the Antarctic middle atmosphere during recurrent geomagnetic storms. Journal of Geophysical Research: Space Physics, 2013, 118, 7874-7885.	2.4	9
139	Techniques to determine the quiet day curve for a long period of subionospheric VLF observations. Radio Science, 2015, 50, 453-468.	1.6	9
140	Magnetic Local Timeâ€Resolved Examination of Radiation Belt Dynamics during Highâ€Speed Solar Wind Speedâ€Triggered Substorm Clusters. Geophysical Research Letters, 2019, 46, 10219-10229.	4.0	9
141	Electron Precipitation From the Outer Radiation Belt During the St. Patrick's Day Storm 2015: Observations, Modeling, and Validation. Journal of Geophysical Research: Space Physics, 2020, 125, e2019JA027725.	2.4	9
142	Linkages Between the Radiation Belts, Polar Atmosphere and Climate: Electron Precipitation Through Wave Particle Interactions. , 2016, , 354-376.		9
143	Investigating radiation belt losses though numerical modelling of precipitating fluxes. Annales Geophysicae, 2004, 22, 3657-3667.	1.6	9
144	Long-term climate change in the D-region. Scientific Reports, 2017, 7, 16683.	3.3	8

#	Article	IF	CITATIONS
145	The effect of snow accumulation on imaging riometer performance. Radio Science, 2000, 35, 1143-1153.	1.6	7
146	Trend and abrupt changes in longâ€ŧerm geomagnetic indices. Journal of Geophysical Research, 2012, 117, ·	3.3	7
147	Dâ€Region High‣atitude Forcing Factors. Journal of Geophysical Research: Space Physics, 2019, 124, 765-781.	2.4	7
148	The Source Regions of Whistlers. Journal of Geophysical Research: Space Physics, 2019, 124, 5082-5096.	2.4	7
149	Demonstrating the Use of a Class of Minâ€Max Smoothers for <i>D</i> Region Event Detection in Narrow Band VLF Phase. Radio Science, 2019, 54, 233-244.	1.6	7
150	Examination of Radiation Belt Dynamics During Substorm Clusters: Activity Drivers and Dependencies of Trapped Flux Enhancements. Journal of Geophysical Research: Space Physics, 2022, 127, .	2.4	7
151	Exceptional middle latitude electron precipitation detected by balloon observations: implications for atmospheric composition. Atmospheric Chemistry and Physics, 2022, 22, 6703-6716.	4.9	7
152	Lower ionosphere monitoring by the South America VLF Network (SAVNET): <i>C</i> region occurrence and atmospheric temperature variability. Journal of Geophysical Research: Space Physics, 2013, 118, 6686-6693.	2.4	6
153	Quiet Daytime Arctic IonosphericDRegion. Journal of Geophysical Research: Space Physics, 2018, 123, 9726-9742.	2.4	6
154	Solar flare Xâ€ r ay impacts on long subionospheric VLF paths. Space Weather, 2021, 19, e2021SW002820.	3.7	6
155	High-latitude geomagnetically induced current events observed on very low frequency radio wave receiver systems. Radio Science, 2010, 45, n/a-n/a.	1.6	5
156	Tropical daytime lower Dâ€region dependence on sunspot number. Journal of Geophysical Research, 2012, 117, .	3.3	5
157	Groundâ€Based Observations of VLF Waves as a Proxy for Satellite Observations: Development of Models Including the Influence of Solar Illumination and Geomagnetic Disturbance Levels. Journal of Geophysical Research: Space Physics, 2019, 124, 2682-2696.	2.4	5
158	Evidence of Subâ€MeV EMICâ€Driven Trapped Electron Flux Dropouts From GPS Observations. Geophysical Research Letters, 2021, 48, e2021GL092664.	4.0	5
159	Cross―Coherence of the Outer Radiation Belt During Storms and the Role of the Plasmapause. Journal of Geophysical Research: Space Physics, 2021, 126, e2021JA029308.	2.4	5
160	What Fraction of the Outer Radiation Belt Relativistic Electron Flux at L â‰^ 3â€4.5 Was Lost to the Atmosphere During the Dropout Event of the St. Patrick's Day Storm of 2015?. Journal of Geophysical Research: Space Physics, 2019, 124, 9537-9551.	2.4	4
161	Simulation study for ground-based Ku-band microwave observations of ozone and hydroxyl in the polar middle atmosphere. Atmospheric Measurement Techniques, 2019, 12, 1375-1392.	3.1	4
162	Comparison of Multiple and Logistic Regression Analyses of Relativistic Electron Flux Enhancement at Geosynchronous Orbit Following Storms. Journal of Geophysical Research: Space Physics, 2019, 124, 10246-10256.	2.4	4

#	Article	IF	CITATIONS
163	Impact of EMICâ€Wave Driven Electron Precipitation on the Radiation Belts and the Atmosphere. Journal of Geophysical Research: Space Physics, 2021, 126, e2020JA028671.	2.4	4
164	Quiet Night Arctic Ionospheric <i>D</i> Region Characteristics. Journal of Geophysical Research: Space Physics, 2021, 126, e2020JA029043.	2.4	4
165	The Effect of Ozone Shadowing on the <i>D</i> Region Ionosphere During Sunrise. Journal of Geophysical Research: Space Physics, 2019, 124, 3729-3742.	2.4	3
166	Spatial Distributions of Nitric Oxide in the Antarctic Wintertime Middle Atmosphere During Geomagnetic Storms. Journal of Geophysical Research: Space Physics, 2020, 125, e2020JA027846.	2.4	3
167	Springâ€Fall Asymmetry in VLF Amplitudes Recorded in the North Atlantic Region: The Fallâ€Effect. Geophysical Research Letters, 2021, 48, e2021GL094581.	4.0	3
168	Impacts of UV Irradiance and Medium-Energy Electron Precipitation on the North Atlantic Oscillation during the 11-Year Solar Cycle. Atmosphere, 2021, 12, 1029.	2.3	3
169	Role of hard X-ray emission in ionospheric D-layer disturbances during solar flares. Earth, Planets and Space, 2022, 74, .	2.5	3
170	The Correspondence Between Sudden Commencements and Geomagnetically Induced Currents: Insights From New Zealand. Space Weather, 2022, 20, .	3.7	3
171	First optical observations of energetic electron precipitation at 4278 Ã caused by a powerful VLF transmitter. Geophysical Research Letters, 2014, 41, 2237-2242.	4.0	2
172	Detecting space weather events with subionospheric VLF observations: Producing quiet day curves from AARDDVARK data. , 2014, , .		1
173	Ground-based very-low-frequency radio wave observations of energetic particle precipitation. , 2020, , 257-277.		1
174	Polar mesosphere summer echo detection using a dynasonde. Radio Science, 2005, 40, n/a-n/a.	1.6	0
175	Unusual observation of chorus at L=2.6. , 2011, , .		Ο
176	Long term determination of variations in energetic electron precipitation into the atmosphere using AARDDVARK. , 2014, , .		0
177	Very Low Latitude Whistlerâ€Mode Signals: Observations at Three Widely Spaced Latitudes. Journal of Geophysical Research: Space Physics, 2019, 124, 9253-9269.	2.4	0
178	Monitoring space weather: using automated, accurate neural network based whistler segmentation for whistler inversion. Space Weather, 0, , .	3.7	0